Annals of Biomedical Engineering
https://doi.org/10.1007/s10439-024-03487-z

BMES BIOMEDICAL ENGINEERING SOCIETY

ORIGINAL ARTICLE

An Experimental Phototherapy Device for Studying the Effects of Blue Light on Patients with Raynaud's Phenomenon

Brett Levac[1] · James Kerber[2] · Emily Wagner[3] · Jerry A. Molitor[4] · Steven S. Saliterman[5]

Received: 25 October 2023 / Accepted: 28 February 2024

Abstract

Raynaud's phenomenon (RP) is a condition that causes decreased blood flow to areas perfused by small blood vessels (e.g., fingers, toes). In severe cases, ulceration, gangrene, and loss of fingers may occur. Most treatments focus on inducing vasorelaxation in affected areas by the way of pharmaceuticals. Recently, animal studies have shown that vasorelaxation can be induced by non-coherent blue light (wavelength ~ 430–460 nm) through the actions of melanopsin, a photoreceptive opsin protein encoded by the *OPN4* gene. To study this effect in humans, a reliable phototherapy device (PTD) is needed. We outline the construction of a PTD to be used in studying blue light effects on Raynaud's patients. Our design addresses user safety, calibration, electromagnetic compatibility/interference (EMC/EMI), and techniques for measuring physiological responses (temperature sensors, laser Doppler flow sensors, infrared thermal imaging of the hands). We tested our device to ensure (1) safe operating conditions, (2) predictable, user-controlled irradiance output levels, (3) an ability for measuring physiological responses, and (4) features necessary to enable a double-blinded crossover study for a clinical trial. We also include in the *Methods* an approved research protocol utilizing our device that may serve as a starting point for clinical study. We introduced a reliable PTD for studying the effects of blue light therapy for patients suffering from Raynaud's phenomenon and showed that our device is safe and reliable and includes the required measurement vectors for tracking treatment effects throughout the duration of a clinical study.

Keywords Raynaud's · Phototherapy · Blue light · Melanopsin · Thermography · Laser doppler flowmetry · Vasorelaxation

Introduction

Raynaud's Phenomenon

Raynaud's phenomenon (RP) is a vasospastic disorder that affects approximately 5% of the population [1, 2] and results in vasoconstriction in the extremities, typically exacerbated by exposure to cold temperatures and/or stress [1–5]. Digital extremities are mostly affected by RP; however, other

Associate Editor Joel Stitzel oversaw the review of this article.

Brett Levac: work was primarily done while a student at the University of Minnesota.

✉ Brett Levac
blevac@utexas.edu

James Kerber
kerbe045@umn.edu

Emily Wagner
wagn0808@umn.edu

Jerry A. Molitor
jmolitor@umn.edu

Steven S. Saliterman
drsteve@umn.edu

[1] Electrical and Computer Engineering, University of Texas at Austin, 2501 Speedway, Austin 78712, USA

[2] University of Minnesota Law School, 229 S 19th Ave, Minneapolis, MN 55455, USA

[3] University of New England, Public Health, 716 Stevens Ave, Portland, ME 04103, USA

[4] University of Minnesota, Scleroderma Clinic, 717 Delaware St. SE, Minneapolis, MN 55414, USA

[5] Biomedical Engineering, University of Minnesota, 312 Church St. S.E. Ste 7-105, Minneapolis, MN 55455, USA

Published online: 26 March 2024

vascular beds can also be disrupted. RP is classified into two different subcategories—primary and secondary RP [6]. Primary RP occurs independently and is thought to have a genetic component. Secondary RP results from underlying conditions, such as an autoimmune disorder [7], other vascular disorders, drug therapies [8, 9], or external repeated trauma such as vibration white finger [10]. In the traditional clinical picture, RP attacks are triphasic, with each phase being distinguishable by skin color of the affected extremities [11]. The initial pallor is the ischemic phase, followed by deoxygenation which causes the skin to turn blue/purple. The final stage is hyperemia and results in red skin color. RP attacks can be severely painful and have associated paresthesia as well [8]. Quality of life can be significantly impacted by RP, and a survey conducted with 443 subjects from varying countries found that 71% of primary RP patients and 87% of secondary RP patients cited a decreased quality of life [12]. Additionally, RP episodes can result in lasting damage to the affected tissues. Complications from RP include digital ulceration [13], digital ischemia, and digital gangrene, and in severe cases, it can result in digit loss [3, 14].

Quantifying Symptoms

To determine the severity of RP in individual patients, it is common to use a Raynaud's Condition Score (RCS) [15, 16]. This is a questionnaire which asks patients to rank the severity of discomfort on a numerical scale. New quantitative metrics such as infrared thermography [17–19] and finger skin thermometry [20] have also been used to verify the presence of RP. Additionally, laser Doppler flowmetry (LDF) has been used to analyze vasodilation in RP patients receiving novel RP treatments [21, 22]. Capillaroscopy, which allows a semi-quantitative assessment of the vascular abnormalities of RP, has been increasingly used to study and understand the differences in vasculopathy between primary and secondary RP and has the potential to measure vascular changes as a consequence of treatment [17, 23, 24].

Current Treatment

Previous approaches to treat RP have been primarily focused on symptom management. There have been recent studies on pharmaceutical approaches such as calcium channel blockers, angiotensin-converting enzyme (ACE) inhibitors, alpha blockers, prostaglandin/prostacyclin analogues, thromboxane synthase inhibitors, selective serotonin reuptake inhibitors, nitrate derivatives, and phosphodiesterase inhibitors, but their success is limited [25–27]. As pharmacologic treatments are systemic, the affected tissues are not solely targeted. These options can have side effects including headaches, ankle swelling, dizziness, palpitations, and flushing. Between the high variability in efficacy and side effects, the clinical utility of these approaches is quite limited. There are other options that offer symptomatic care to the Raynaud's affected tissues. However, these typically operate by applying heat [28, 29] which can be difficult to reliably localize and regulate the applied temperature. There are also techniques which seek to treat the resulting digital ulcers after formation but do not serve as a preventative measure to protect against ulcer formation [13]. Recently, there have been studies which look to analyze the effectiveness of iloprost infusion in patients by evaluating blood flow using LDF [21, 24]. This study showed increased blood flow following 3 days of infusions, but flow benefits faded shortly after treatment.

Motivating Work

Sikka et al. described achieving photorelaxation by the application of blue light (455 nm) to the mice tail artery [30]. They reported the presence of melanopsin (opsin4; Opn4) in blood vessels and its ability to mediate wavelength-specific light-dependent vascular relaxation. Their group subsequently demonstrated that Opsin3 and Opsin4 mediate photorelaxation through G protein-coupled receptor kinase2 (GRK2) and that GRK2 inhibition could amplify blue light-mediated photorelaxation and prevent physiological desensitization to repeated blue light exposure [31]. Opsins are photoreceptor molecules originally identified in the retinal cells. These proteins can change their conformation from a resting state to a signaling state upon light activation. In so doing, they activate G protein-coupled receptors (GPCR) in the cellular membrane, thereby converting an extracellular signal into an intracellular response.

Light therapy has been under investigation and in clinical use for a variety of conditions [32–37]; blue light exposure has shown promise in other settings such as decreasing systolic blood pressure and arterial stiffness [33] and also treating neonatal jaundice [34]. Recent studies have investigated the efficacy of low levels of light therapy for systemic sclerosis digital ulcers. In an open-label trial using light-emitting diodes of wavelengths of 850 nm, 660 nm, and 405 nm delivered simultaneously, the pain visual analogue score (VAS) of patients' painful ulcers showed significant improvement post-treatment [22]. It is important to note that this device delivered localized light therapy to digits with ischemic ulcers, rather than delivering light therapy to the entire hand. Additionally, the study was not done to measure a response to RP per se and did not incorporate blue light at the frequency investigated here in an attempt to harness Opsin4-mediated photorelaxation.

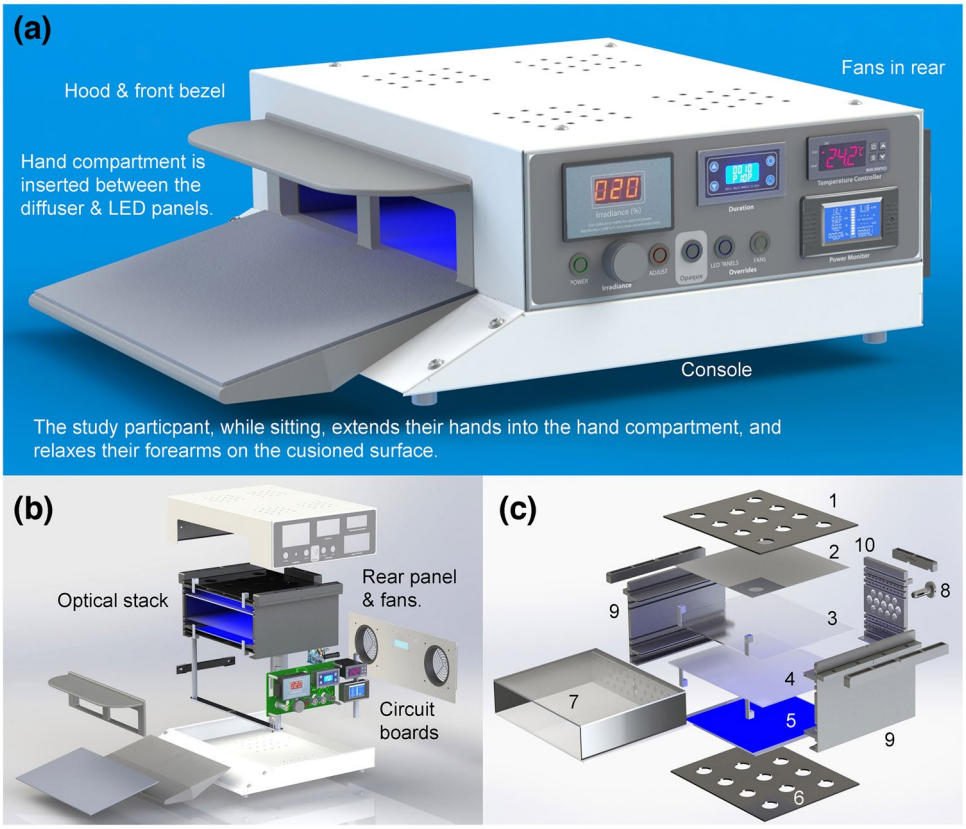

Fig. 1 **a** PTD rendered in Solidworks *Photorealistic View*. CAD was supplemented with ray-tracing of the blue light from both LED panels to understand the distribution of light within the inner hand compartment (HC), including internal reflections and stray light. (The console operation is explained later.) Light passes from the LED panels, through the light diffuser, through the clear hand compartment and illuminates the hands from above and below. Stray light and reflections are minimized by black vertical surfaces. **b** The PTD enclosure is a powder-coated, all-steel unit with ventilated top and bottom sections; an optical stack, custom circuit boards, carry handle, hood & front bezel, cushioned forearm rest, and fans on the back panel. **c** The removable optical stack is also a ventilated enclosure fabricated from acrylic and PLA, with side-wall channels for inserting the LED panels, diffusers and HC. Shown are the fixed & vented cover (1), upper blue LED panel (2) , upper microbead light diffuser (3), lower diffuser (4), lower LED panel (5), fixed bottom (6), HC (7) that slides into place and is illuminated from above and below by the two LED panels, fixed rear thermocouple probe (8) that automatically enters the HC upon insertion, and side (9) and back walls (10) that hold the stack together and allow the other panels to be easily slid into place. The optical stack is only removed from the cabinet for servicing.

Materials and Methods

Considerations for Experimental PTD

When building an experimental PTD, there are several important considerations which must be addressed. Firstly, there must be a guarantee of safe operating conditions for both the subject and any device operator (i.e., electrical safety, hygiene standards, etc.). Next, to properly administer set treatment levels, there must be predictable, user-controlled irradiance output settings that can be reliably maintained during device operation. Additionally, there should be an ability to measure physiological responses to treatment through a diverse set of measurement techniques. Finally, it is necessary to include device features which enable a double-blinded crossover study for clinical trials.

Device Overview

The PTD is composed of an outer enclosure, optical stack, circuit board, and a rear panel containing power inputs and cooling fans. The fully assembled PTD and exploded views of the assembly are shown in Fig. 1. The patient only makes contact with the removable hand compartments (HC) made of acrylic. This isolates the user from the inner workings of the unit (Fig. 2). One compartment is clear to allow blue light to pass from above and below (treatment), and the other is opaque with reflective mylar that blocks all blue light incident on its surface (sham). Blue light generated by the two LED panels passes through

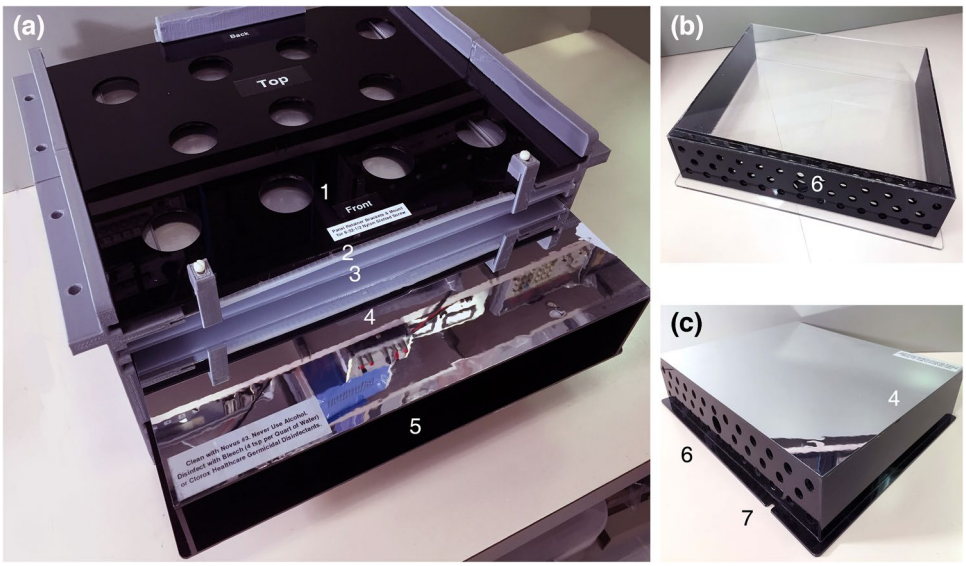

Fig. 2 **a** Photograph of the optical stack with hand compartment (HC) partially extended. Shown are the, fixed & vented cover (1), LED panel slid into place (2), microbead diffuser slid into place (3), reflective Mylar surface on sham (opaque) HC (4), and sham (opaque) HC front opening for insertion of participant hands (slid forward for better viewing) (5). **b** Rear-view of the clear acrylic HC. Shown is a large hole for automatic insertion of the thermocouple temperature probe as the hand compartment is slid into place (6), and **c** Rear-view of the sham HC showing reflective surface (4), temperature probe hole (6) and rear notch (7) for sensing and determining which hand compartment is inserted. If no hand compartment is detected, power is shut-off to the entire system for safety.

diffusers (Acrylite microbead acrylic Satinize Light Diffuser, 0D010 DF) then to the HC. For safety, the inside surface of each of HC can be easily disinfected with Clorox® wipes by simply removing the HC from the larger assembly. A front bezel with hood, along with blue-blocking eyewear (Uvex S0360X), protects the participant and research assistant (RA) from any long-term effects of blue light [38].

To reduce heating, muffin fans are placed behind the PTD to gently pull air into and through the entire unit, exiting in the rear. Air movement is not sensed by the study participant. The electronics are also ventilated. The HC rear panels have offset ventilation holes (to minimize stray light), and a single port for a temperature sensor holder (larger hole in center). The reflective mylar prevents unwanted heating of the opaque HC. (This was determined experimentally and verified by thermal imaging of the inside surface of the HC). The notch visible on the rear-edge (Fig. 2c) is sensed by a microswitch inside the PTD to determine which HC is present. An automatic shutoff prevents operation of the unit when no hand compartment is present (a second microswitch confirms the presence of at least one of the HC). The HC temperature sensor hole is shown in Fig. 1c. Finger skin and ambient room temperatures are displayed and recorded (Omega Temperature Data Logger). The temperature within the PTD itself (aside from the HC) may be monitored by the research assistant on a digital display located on the console on the right side of the PTD.

When a double-blinded crossover protocol is performed in a clinical study, neither the participant nor RA conducting the study is aware which HC is being used. Unblinded personnel configure the PTD for the given session by temporarily removing the PTD front bezel and changing HCs.

LED Panels

The phototherapy device contains two separate blue LED panels (Yescom, 225 LEDs, wavelength 453 nm). These are positioned above and below the hand compartment and are separated by a diffuser as shown in Fig. 1c. The operational wavelength of the panels is within the prescribed range suggested by the previous work [30, 31] and their irradiance levels ensure diffusion of light through skin [35, 39–41]. Both LED panels and the diffusers reside in a larger assembly called the optical stack. The optical stack is a stable and removable subassembly which allows for easy insertion and removal of the hand compartment through the front of the PTD (Fig. 1c).

Light Energy and Limits of Exposure

The limit for skin exposure at a wavelength of 453 nm, which considers the duration of the exposure [42], is the following energy density:

Fig. 3 The PTD console is located on the PTD's right side and is not visible to a study participant. Irradiance (mW/m^2) and duration of exposure are set based on a study protocol. Irradiance (as a percent PWM) is determined in advance from the power level calibration chart for the installed LED panels. The hand compartment temperature, and operating parameters are also displayed to verify the system is operating within specifications. The opaque compartment indicator light is inactivated in a double-blinded study.

$$500\frac{\text{Joules(J)}}{\text{cm}^2} = \frac{energy}{unit\ area}$$

Each PTD LED panel generates the following energy flux (Fig. 7c):

$$3500\frac{\text{milliwatt}}{m^2} = 3.5\frac{\text{Watt(W)}}{\text{m}^2} = \frac{rate\ of\ energy\ transfer}{unit\ area}$$

and given

$$1\text{W} = 1\frac{\text{J}}{\text{s}} or 1\text{J} = 1\text{Ws}, \text{and} 1\frac{\text{W}}{\text{m}^2} = 10^{-4}\frac{\text{W}}{\text{cm}^2}$$

then for a duration of, e.g., 30 minutes, or 1800 seconds, the following is the energy density:

$$3.5 \times 10^{-4}\frac{\text{W}}{\text{cm}^2} \times 1800\text{s} \times \frac{1\text{J}}{1Ws} = .630\frac{\text{J}}{\text{cm}^2}$$

which is well below the limit.

The exposure duration is set by an electronic timer on the console and is programmed in advance. Recalibration requires placing the machine in calibration mode and uses of a physical key to access.

Operation

The research assistant operates the PTD from the console on the right side of the PTD. Blue light treatment duration and the irradiance level are set as specified by the clinical study protocol (Fig. 3). The temperature is set to room temperature to provide a stable hand compartment temperature. Integration of the console and electronic subsystems is described in the Appendix, Fig. 8.

EMC/EMI

Electromagnetic compatibility (EMC) and electromagnetic interference (EMI) were considered during the design and testing of the PTD. EMC is the ability of the PTD to function acceptably in the proposed electromagnetic environment. EMI is unwanted noise or interference to the electrical paths or circuits caused by an outside source.

As an experimental and not commercial device, our attention turned to assuring the device did not emit electromagnetic interference that would affect its operation, including the sensors.

Sources of EMI include the displays, indicators and switches, circuit boards, electrical cabling, LED panels, and interconnecting leads to sensors and recording equipment. EMI was tested by using a spectrum analyzer and near-field probes. Suspected emission sources were shielded as best as possible with grounded aluminum or steel enclosures. Aluminum works for electrical fields, and steel is necessary for magnetic fields (e.g., fields radiated by inductors). Magnetic waves cannot be grounded or blocked but can be redirected by high permeability metals such as steel or mu-metal.

We initially observed instability of the thermocouple baseline readings which were due to EMI from the LED panels. Thus, we switched to RTD sensors which have better immunity to EMI, and this alteration resolved the problem. (Guidance for assessing EMC in a commercial product can be obtained from the US Food and Drug Administration (FDA) which regulates medical devices and the US Federal Communications Commission (FCC).)

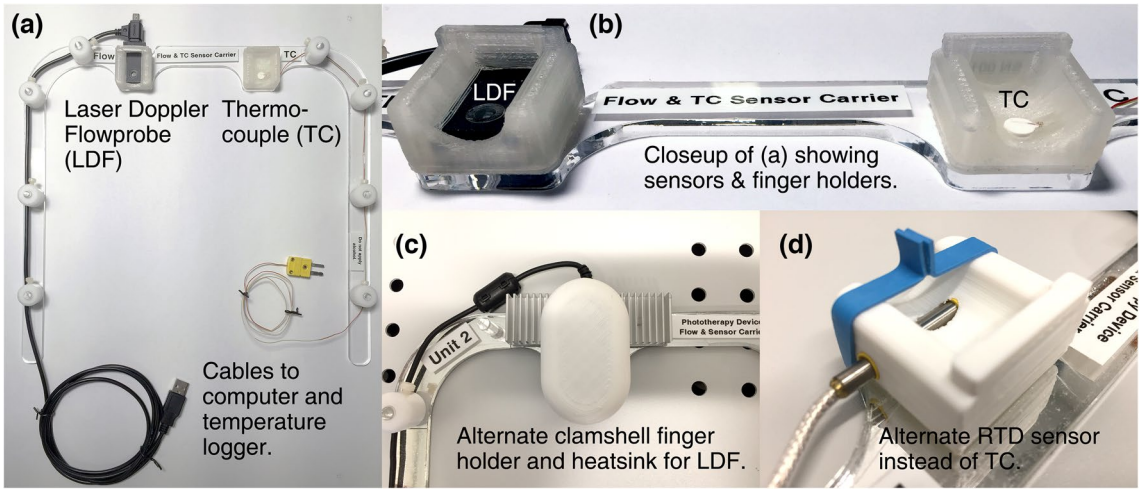

Fig. 4 Photographs of **a** removable sensor carrier, **b** closeup of **a** showing the laser doppler flowmeter (LDF) and thermocouple sensors, and finger holders, **c** optional clamshell-style LDF sensor holder (the finger is slid under the spring-loaded cover), and **d** preferred RTD temperature sensor with elastic band. Variations of the carrier and finger holders were tested to improve the user experience.

Assessing Microcirculation

Symptoms reported by a study participant, quantified by the VAS, are the most important measure of the effectiveness of blue light therapy for RP patients (Sec. 1.2). However, measuring physiologic parameters such as skin temperature and LDF during operation of the PTD, as well as thermal imaging before and after a study session are potentially helpful. It is important to note that the latter are all affected by natural variations in vascular physiology from person to person and can be misleading so care must be taken when building conclusions upon their absolute values. Variables such as time of season, room temperature, physical conditioning, activity before testing, diet, acclimation time to the test room, medications, clothing, and age may affect both the baseline and test readings. All of these issues were encountered at some point in testing the PTD and need to be considered when designing a study protocol.

A U-shaped carrier for sensors to measure finger skin temperature and LDF was constructed, along with custom sensor holders (Fig. 4). This is conveniently placed into the HC where readings can be taken continuously throughout the treatment. The leads are fixed to the edges of the carrier minimizing contact with the hands.

Laser Doppler Flowmetry

Blood flow can be measured continuously in a single finger (Fig. 4) of the participant during a study using an LDF sensor (Kyocera Corp.). Data are captured on a computer for later analysis. LDF measures shifts in optical signals which occur when coherent light is transmitted into tissue and photons are scattered by moving objects [43, 44]. The returning photon frequency will be modified if they encounter moving particles due to the Doppler effect [43]. The purpose is to look for changes in circulation and to compare between blue light exposure vs. sham therapy. LDF has been used to assess microcirculation before [45].

Continuous LDF readings were found to be marginally useful because of inherent variability of the readings related to contact pressure (finger to sensor). Several techniques were investigated to ensure proper contact pressure such as the use of a sensor clamshell finger holder. Unfortunately, this proved to be no better than simply resting the finger in a custom holder. However, an added elastic band over the holder did improve the recordings and was adopted for all future readings. Another problem discovered was heating of the sensor by its own electronics over time, giving a false reading of increased flow. To minimize this effect, the LDF sensor was mounted on a heatsink (Fig. 4c). There was no reliable method to calibrate readings; therefore, only relative comparisons were possible. LDF sensors from other manufacturers may prove more useful. An alternative and perhaps preferable approach is to use LDF before and after a session, outside of the PTD [22].

Skin Temperature

Finger skin temperature is obtained by having the participant place their right middle finger in the holder shown in Fig. 4c,d. Skin, HC, and ambient room temperatures are all recorded simultaneously with RTD sensors and recorded (Omega Temperature Data Logger).

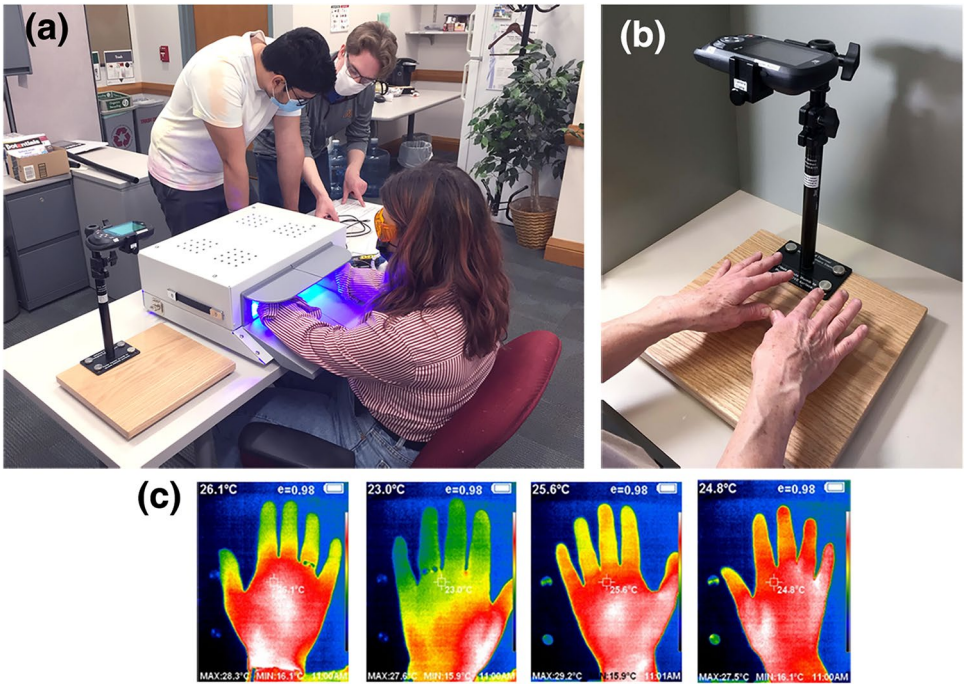

Fig. 5 **a** Testing session with contributor Sehgal (left), and authors Kerber and Wagner (foreground). **b** Thermal imaging camera (Hti HT-A2) and custom stand. Images are obtained of the dorsal and palmar surfaces of the hands while they are held above the base of the stand. (Resting the hands on the base would alter their temperature.) **c** Representative baseline images - palmar and dorsal surfaces, left and right hands. The thermal images show temperature as a false-color gradient (a spectrum bar is visible on the right-hand side of the images), based on the minimum and maximum temperatures recorded and displayed at the bottom of the images. More useful for study purposes is the ability to sample any point in the image using an adjustable cursor, allowing measurement to 0.1 °C over specific anatomical landmarks as specified by the clinical study protocol. This measurement is shown in the upper left-hand corner of the image. Study participant data based on use of the PTD is deferred to a future clinical study and will be the subject of another paper.

Thermal imaging

Thermal imaging with an infrared camera (Hti HT-A2) offered another assessment of circulation in the hands, subject to the limitations described in the introduction to this section. Fig. 5 shows the thermal imaging camera (Hti HT-A2) and representative baseline images.

Visual Analogue Score (VAS) and Clinical Study

Clinical study requires the use of the pain visual analogue score (VAS) for participants to score the severity of their symptoms before and after treatment, employing a cold room or cold-water immersion to provoke a vasospastic event, and using either blue light exposure or sham based on the procedural steps shown in Fig. 6. The procedural steps below are repeated several times in the course of a study participant session. The VAS is the means by which clinical investigators will be able to compare this treatment with traditional treatments.

For the study to be double-blinded, unblinded personnel configure the equipment in advance, and a blinded RA conducts the study in the presence of the blinded study participant. Both the participant and RA wear blue-blocking eyewear. To complete the crossover, the study is repeated but with the hand compartments swapped between sessions (following a washout period to avoid carryover effects). The design choices present in our PTD enable a safe, easy, and repeatable implementation of such a protocol.

Results

Calibration of LED Panels

The LED panels have a fixed voltage requirement and compliant current based on the irradiance setting. Irradiance (mW/m^2) is adjusted by using pulse width pulse modulation (PWM), a customary method for dimming LEDs. Measurements were obtained at five locations over the LED panel and averaged (Fig. 7a). Irradiance was plotted against a PWM setting (0-100% in 10% increments) and found to have a linear relationship (Fig. 7c). Calibration controls are accessed through a secure opening on the back of the PTD.

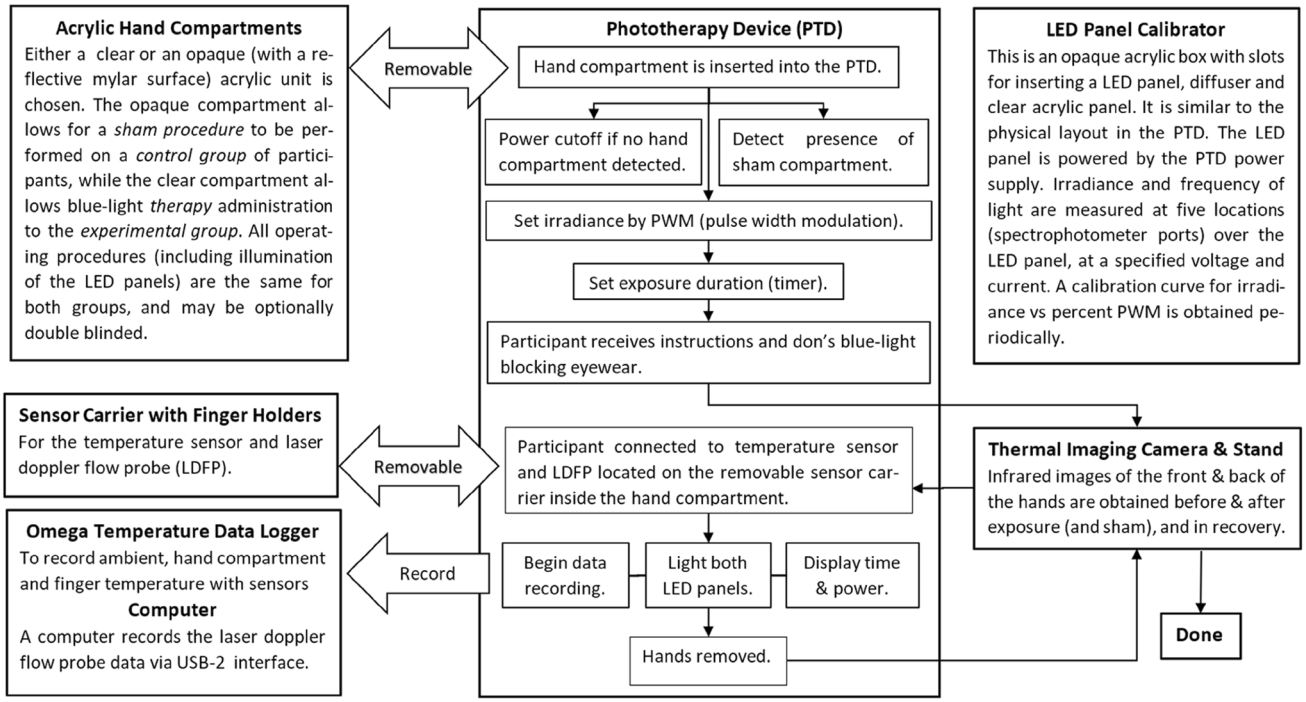

Fig. 6 Proposed procedural steps for operating the PTD during a clinical study. The actual study protocol will require additional steps of repeated cold exposure, runs with the PTD (as above), and symptom severity surveys.

Testing

Several practice sessions with the PTD were done to test functionality, EMI, sensor configuration, human machine interface, and suitability for study participants. The human machine interface refers to those features, such as the console, computer, software, and external temperature logger, that enable the personnel to control the machine. Some of the changes included the addition of an armrest cushion, added EMI shielding inside the PTD, and investigation of other sensor options.

Discussion

We have demonstrated that our device exhibits (1) safe operating conditions for a study participant, (2) predictable, user-controlled irradiance output levels with a custom calibration-assist device, (3) an ability for measuring physiological responses (with limitations), and (4) features necessary to enable a double-blinded crossover study for a clinical trial. To show how our device can be used in a proper clinical study, we designed a double-blinded crossover protocol that has been approved for human subjects (University of Minnesota IRB) and will be the subject of a future paper.

In summary, when used in a safe manner, an effective means for studying the effect of blue light irradiance of the hands in patients with RP has been achieved with our device. The use of blue light therapy, either alone or in combination with pharmaceutical agents, delivered by stationary (derived from this PTD) or mobile medical devices (e.g., gloves with embedded light sources) may potentially improve the quality of life of patients who suffer from RP and similar vasospastic disorders.

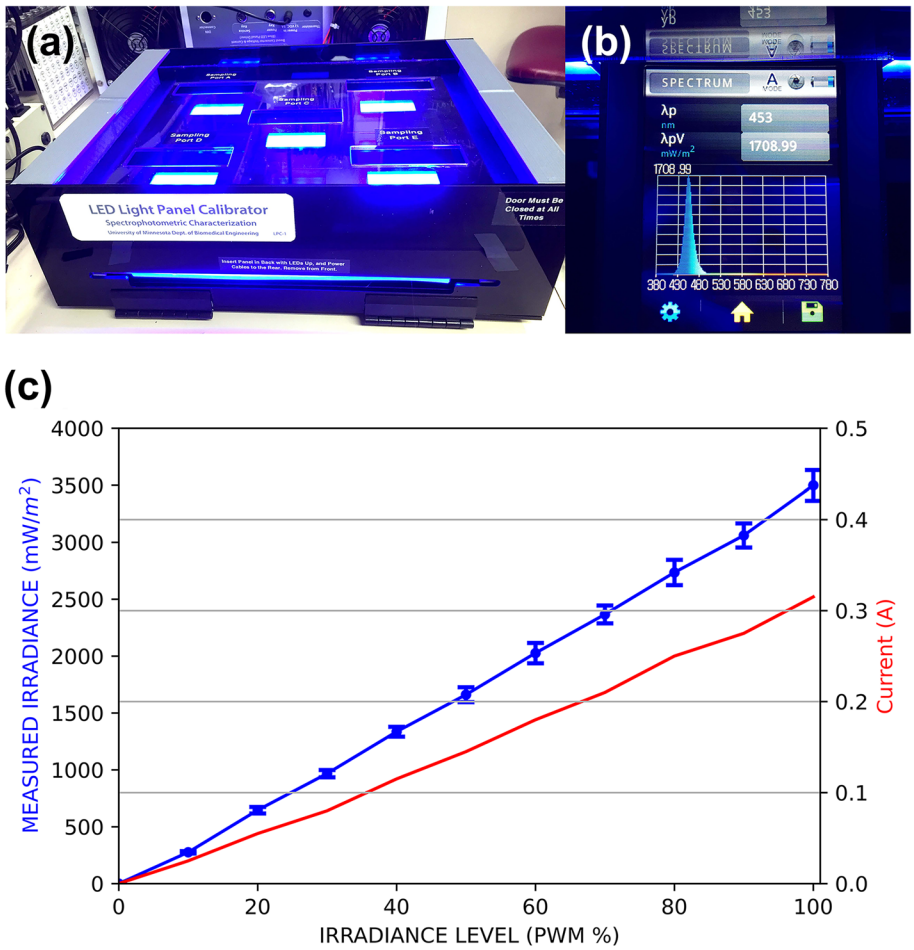

Fig. 7 **a** The custom calibration-assist device was constructed similar to the PTD optical stack (Fig 2b), but containing only one diffuser, an acrylic plate representing the top or bottom of the HC, and two acrylic plates that position the spectroradiometer above the light source. The distance from the LED panel to the meter, and intervening light absorbing materials, replicates the PTD optical stack. The test LED panel is inserted into an opening in front of the calibrator. **b** The spectroradiometer (UPRtek/ Gamma Scientific MK350N) is shown here (inverted for readability) plugged into a test port. A total of 55 samples were obtained for each panel − 11 readings for each sampling location. The spectral power distribution (graph of energy levels vs wavelength) is shown, and peak wavelength and irradiance are displayed numerically. Ordinarily calibration is performed in a dark room and removable plugs are placed into the open ports. The same device can be used to measure the light absorption of a specific material (e.g., the diffuser), by first characterizing the light source without any intervening material, then repeating with the material in place. **c** Calibration curves for one of two required LED panels. Irradiance (mW/m^2) is plotted against the PWM setting. There is some variation in power level based on sampling location over the panel, and the five sampling locations are averaged. The standard deviation between the spatial locations is also included as error bars on the plot. Additionally, current draw was found to be linear with changing PWM levels. Voltage is regulated (fixed).

As with any device used with human subjects, diligence with repeated calibration, monitoring of internal systems, assessing and recording of reported problems, and addressing matters of safety—including irradiance, automatic power shutoff, and sanitation are paramount. Study protocols should incorporate a second research assistance for double-checking settings.

Appendix

Electronic Subsystems

See Fig. 8.

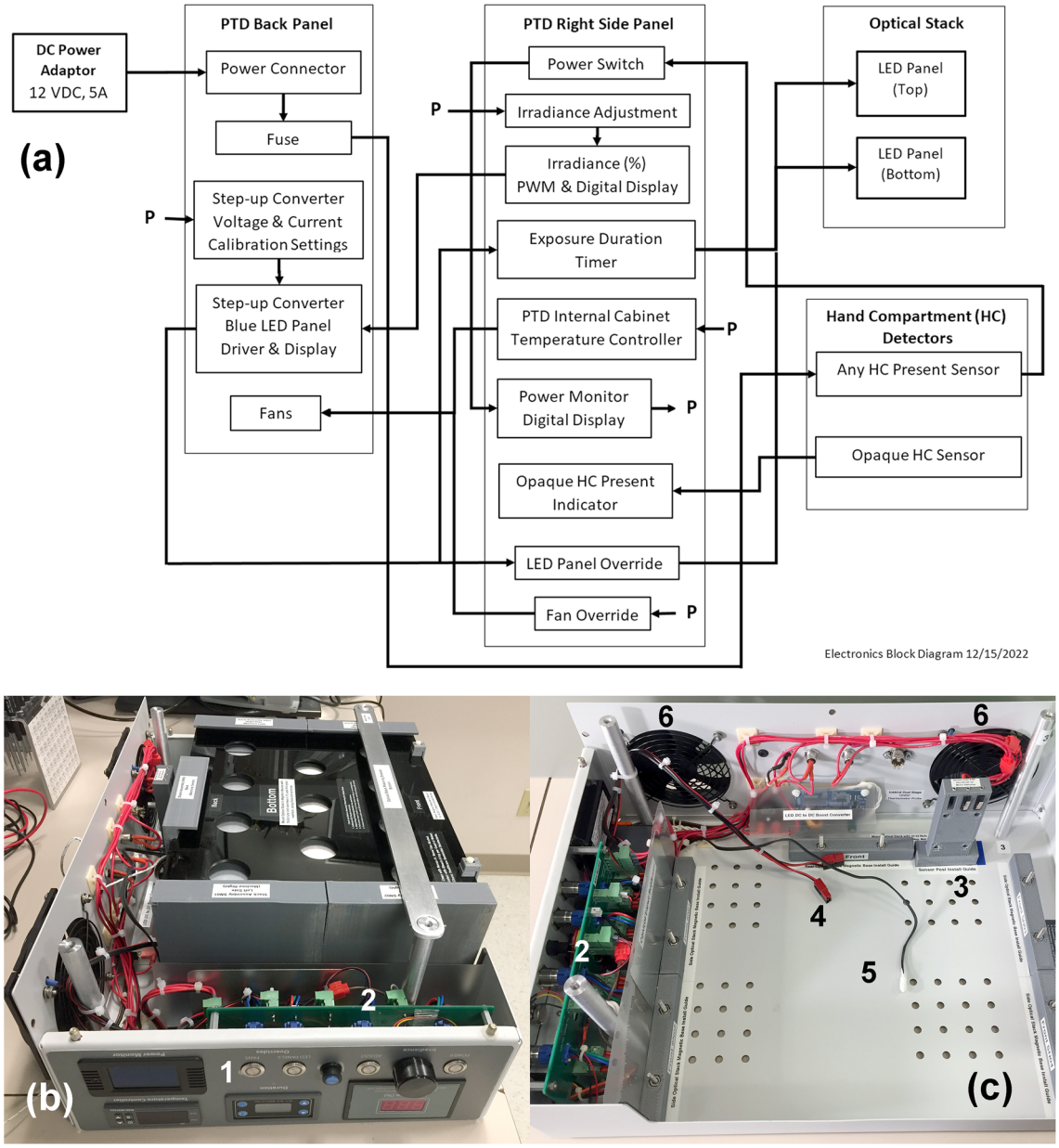

Fig. 8 **a** Integration of the PTD console, optical stack and electronic subsystems as viewed from the bottom. 12 VDC from the power monitor is distributed to the various units as shown (letter P). A step-up converter brings the 12 VDC power supply to ~ 42 VDC for the LED panels. This voltage is adjustable and set at the time of calibration. **b** Bottom view. A custom PCB (1) was created for interconnecting the various displays, indicator lights, fans, switches (1, 2), LED panels, power supply, and fuse. **c** Bottom view with optical stack and shielding removed for visibility. The HC detector microswitches (3), LED power connector (4), HC thermocouple (5) and fans (6) can be seen. The TC is fastened into a holder attached to the back of the optical stack, allowing it to extend into an inserted HC automatically (see Fig. 1c). The HC can then be changed for treatment vs. sham studies without needing to reconnect the thermocouple.

Acknowledgments The authors acknowledge the participation and invaluable contributions of Jennifer Chmura and Kushal Sehgal. We are also grateful for support from the University of Minnesota Institute for Engineering in Medicine (IEM).

Declarations

Disclosures On January 9, 2024 the authors and the University of Minnesota received a patent (U.S. 11,865,357) for the PTD and various methods for translating the technology into useful solutions for patients (both stationary and wearable systems).

References

1. Herrick, A. L. Raynaud's phenomenon. *J. Scleroderm. Relat. Disord.* 4:89–101, 2019. https://doi.org/10.1177/2397198319826467.
2. Haque, A., and M. Hughes. Raynaud's phenomenon. *Clin. Med. (Northfield Il).* 20:580–589, 2020. https://doi.org/10.7861/clinmed.2020-0754.
3. Silva, I., G. Teixeira, M. Bertão, R. Almeida, A. Mansilha, and C. Vasconcelos. Raynaud phenomenon. *Rev. Vasc. Medi* 4–5:9–16, 2016. https://doi.org/10.1016/j.rvm.2016.03.001.
4. White, R. Z., T. Nguyen, and M. J. Sampson. Magnetic resonance characterisation of primary Raynaud's phenomenon. *J. Med. Imaging Radiat. Oncol.* 2021. https://doi.org/10.1111/1754-9485.13293.
5. Herrick, A. L., and F. M. Wigley. Raynaud's phenomenon. *Best Pract. Res. Clin. Rheumatol.* 34:101474, 2020. https://doi.org/10.1016/j.berh.2019.101474.
6. Murphy, S. L., A. Lescoat, M. Alore, et al. How do patients define Raynaud's phenomenon? Differences between primary and secondary disease. *Clin. Rheumatol.* 40:1611–1616, 2021. https://doi.org/10.1007/s10067-021-05598-7.
7. Shtefiuk, O. V., R. I. Yatsyshyn, P. R. Herych, Y. Y. Karpyuk, and V. B. Boychuk. Features of the Raynaud's syndrome course in patients with rheumatoid arthritis. *World Med. Biol.* 71:145–149, 2020. https://doi.org/10.26724/2079-8334-2019-4-70-145-149.
8. Devgire, V., and M. Hughes. Raynaud's phenomenon. *Br. J. Hosp. Med.* 80:658–664, 2019. https://doi.org/10.12968/hmed.2019.80.11.658.
9. Rogers, S., and M. Hughes. Digital artery vasospasm in primary Raynaud's phenomenon. *Eur. J. Rheumatol.* 7:201–202, 2020. https://doi.org/10.5152/eurjrheum.2020.19211.
10. Vihlborg, P., K. Makdomi, H. Gavlovska, S. Wikstrom, and P. Graff. Arterial abnormalities in the hands of workers with vibration white fingers - a magnetic resonance angiography case series. *J. Occup. Med. Toxicol.* 16:27, 2021. https://doi.org/10.1186/s12995-021-00319-x.
11. Choi, E., and S. Henkin. Raynaud's phenomenon and related vasospastic disorders. *Vasc. Med.* 26:56–70, 2021. https://doi.org/10.1177/1358863x20983455.
12. Hughes, M. Assessment and management of Raynaud's phenomenon. *Prescriber.* 28:11–16, 2017.
13. Sato, T., K. Arai, and S. Ichioka. Hyperbaric oxygen therapy for digital ulcers due to Raynaud's disease. *Case Rep. Plast. Surg. Hand Surg.* 5:72–74, 2018. https://doi.org/10.1080/23320885.2018.1525684.
14. Pauling, J. D., M. Hughes, and J. E. Pope. Raynaud's phenomenon-an update on diagnosis, classification and management. *Clin. Rheumatol.* 38:3317–3330, 2019. https://doi.org/10.1007/s10067-019-04745-5.
15. Herrick, A. L., C. Heal, J. Wilkinson, et al. Temperature response to cold challenge and mobile phone thermography as outcome measures for systemic sclerosis-related Raynaud's phenomenon. *Scand. J. Rheumatol.* 2021. https://doi.org/10.1080/03009742.2021.1907926.
16. Merkel, P. A., K. Herlyn, R. W. Martin, et al. Measuring disease activity and functional status in patients with scleroderma and Raynaud's phenomenon. *Arthritis Rheum.* 46:2410–2420, 2002. https://doi.org/10.1002/art.10486.
17. Sternbersky, J., M. Tichy, and J. Zapletalova. Infrared thermography and capillaroscopy in the diagnosis of Raynaud's phenomenon. *Biomed. Papers-Olomouc.* 165:90–98, 2021. https://doi.org/10.5507/bp.2020.031.
18. Lindberg, L., B. Kristensen, E. Eldrup, J. F. Thomsen, and L. T. Jensen. Infrared thermography as a method of verification in Raynaud's phenomenon. *Diagnostics.* 11:981, 2021. https://doi.org/10.3390/diagnostics11060981.
19. Lindberg, L., B. Kristensen, J. F. Thomsen, E. Eldrup, and L. T. Jensen. Characteristic features of infrared thermographic imaging in primary Raynaud's phenomenon. *Diagnostics.* 11:558, 2021. https://doi.org/10.3390/diagnostics11030558.
20. Aleksiev, T., Z. Ivanova, H. Dobrev, and N. Atanasov. Application of a novel finger temperature device in the assessment of subjects with Raynaud's phenomenon. *Skin Res. Technol.* 2021. https://doi.org/10.1111/srt.13070.
21. Rotondo, C., M. Nivuori, A. Chialà, et al. Evidence for increase in finger blood flow, evaluated by laser Doppler flowmetry, following iloprost infusion in patients with systemic sclerosis: a week-long observational longitudinal study. *Scand. J. Rheumatol.* 47:311–318, 2018. https://doi.org/10.1080/03009742.2017.1397187.
22. Hughes, M., T. Moore, J. Manning, et al. A feasibility study of a novel low-level light therapy for digital ulcers in systemic sclerosis. *J. Dermatol. Treat.* 30:251–257, 2019. https://doi.org/10.1080/09546634.2018.1484875.
23. Ingegnoli, F., V. Smith, A. Sulli, and M. Cutolo. Capillaroscopy in routine diagnostics: potentials and limitations. *Curr. Rheumatol. Rev.* 14:5–11, 2018. https://doi.org/10.2174/1573397113666170615084229.
24. Herrick, A. L., M. Berks, and C. J. Taylor. Quantitative nailfold capillaroscopy-update and possible next steps. *Rheumatology.* 60:2054–2065, 2021. https://doi.org/10.1093/rheumatology/keab006.
25. Su, K. Y. C., M. Sharma, H. J. Kim, et al. Vasodilators for primary Raynaud's phenomenon. *Cochrane Database Syst Rev.* 2021. https://doi.org/10.1002/14651858.CD006687.pub4.
26. Thompson, A. E., and J. E. Pope. Calcium channel blockers for primary Raynaud's phenomenon: a meta-analysis. *Rheumatology.* 44:145–150, 2005. https://doi.org/10.1093/rheumatology/keh390.
27. Wigley, F. M., and N. A. Flavahan. Raynaud's phenomenon. *N Engl. J. Ed.* 375:556–565, 2016. https://doi.org/10.1056/NEJMra1507638.
28. Dawit, H. W., Q. Zhang, Y. M. Li, S. R. Islam, J. F. Mao, and L. Wang. Design of electro-thermal glove with sensor function for Raynaud's phenomenon patients. *Materials.* 14:377, 2021. https://doi.org/10.3390/ma14020377.
29. Azuma, N., T. Furukawa, Y. Shima, and K. Matsui. A usability survey of wrist mounted disposable heat pad on Raynaud's phenomenon in patients with connective tissue diseases. *Ann Rheum Dis.* 79:692–693, 2020. https://doi.org/10.1136/annrheumdis-2020-eular.443.
30. Sikka, G., G. P. Hussmann, D. Pandey, et al. Melanopsin mediates light-dependent relaxation in blood vessels. *Proc. Natl. Acad. Sci. USA* 111:17977–17982, 2014. https://doi.org/10.1073/pnas.1420258111.
31. Ortiz, S. B., D. Hori, Y. Nomura, et al. Opsin 3 and 4 mediate light-induced pulmonary vasorelaxation that is potentiated by G protein-coupled receptor kinase 2 inhibition. *Am. J. Physiol.* 314:L93–L106, 2018. https://doi.org/10.1152/ajplung.00091.2017.
32. Modi, P., K. Jha, Y. Kumar, T. Kumar, R. Singh, and A. Mishra. The effect of short-term exposure to red and blue light on the autonomic tone of the individuals with newly diagnosed essential hypertension. *J. Fam. Med. Primary Care.* 8:14–21, 2019. https://doi.org/10.4103/jfmpc.jfmpc_375_18.
33. Stern, M., M. Broja, R. Sansone, et al. Blue light exposure decreases systolic blood pressure, arterial stiffness, and improves endothelial function in humans. Randomized Controlled Trial Research Support, Non-U.S. Gov't. *Eur. J. Prevent. Cardiol.*. 25:1875–1883, 2018. doi:https://doi.org/10.1177/2047487318800072

34. Montealegre, A., N. Charpak, A. Parra, C. Devia, I. Coca, and A. M. Bertolotto. Effectiveness and safety of two phototherapy devices for the humanised management of neonatal jaundice. *Anal Pediatr.* 92:79–87, 2020. https://doi.org/10.1016/j.anpedi.2019.02.008.
35. Liu, B. C., T. J. Farrell, and M. S. Patterson. Comparison of photodynamic therapy with different excitation wavelengths using a dynamic model of aminolevulinic acid-photodynamic therapy of human skin. *J. Biomed. Opt.* 17:088001, 2012. https://doi.org/10.1117/1.Jbo.17.8.088001.
36. Kleinpenning, M. M., M. E. Otero, P. E. J. van Erp, M. J. P. Gerritsen, and P. C. M. van de Kerkhof. Efficacy of blue light vs. red light in the treatment of psoriasis: a double-blind, randomized comparative study. *J Eur Acad Dermatol Venereol.* 26:219–225, 2012. https://doi.org/10.1111/j.1468-3083.2011.04039.x.
37. Keemss. Prospective, randomized study on the efficacy and safety of local UV-free blue light treatment of eczema (vol 232, pg 496, 2016). *Dermatology*. 232:522–522, 2016.
38. Shang, Y. M., G. S. Wang, D. H. Sliney, C. H. Yang, and L. L. Lee. Light-emitting-diode induced retinal damage and its wavelength dependency in vivo. *Int. J. Ophthalmol.* 10:191–202, 2017. https://doi.org/10.18240/ijo.2017.02.03.
39. Schmitt, J. M., G. X. Zhou, E. C. Walker, and R. T. Wall. Multilayer model of photon diffusion in skin. *J. Opt. Soc. Am. A.* 7:2141–2153, 1990. https://doi.org/10.1364/josaa.7.002141.
40. Lisenko, S. A., M. M. Kugeiko, and A. M. Lisenkova. Noninvasive determination of spectral depth of light penetration into skin. *OptSp.* 115:779–785, 2013. https://doi.org/10.1134/s0030400x13110167.
41. Kim, M., J. An, K. S. Kim, et al. Optical lens-microneedle array for percutaneous light delivery. *Biomed. Opt. Express.* 7:4220–4227, 2016. https://doi.org/10.1364/BOE.7.004220.
42. Liebmann, J., M. Born, and V. Kolb-Bachofen. Blue-light irradiation regulates proliferation and differentiation in human skin cells. *J. Invest. Dermatol.* 130:259–269, 2010. https://doi.org/10.1038/jid.2009.19.
43. Webb, R. C., Y. J. Ma, S. Krishnan, et al. Epidermal devices for noninvasive, precise, and continuous mapping of macrovascular and microvascular blood flow. *Sci. Adv.* 1:e1500701, 2015. https://doi.org/10.1126/sciadv.1500701.
44. Humeau, A., W. Steenbergen, H. Nilsson, and T. Stromberg. Laser Doppler perfusion monitoring and imaging: novel approaches. *Med Biol Eng Comput.* 45:421–435, 2007. https://doi.org/10.1007/s11517-007-0170-5.
45. Nogami, H., K. Komatsutani, T. Hirata and R. Sawada. IEEE TPC. Integrated laser Doppler blood flowmeter combining optical contact force, pp. 287–290, 2019.